25th ABCM International Congress of Mechanical Engineering
October 20-25, 2019, Uberlândia, MG, Brazil

COB-2019-1226
EXPERIMENTAL MEASUREREMENTS ON THE FLOW OVER A SIMPLIFIED NOSE LANDING GEAR

Denner Sávio Santos
Odenir de Almeida
Federal University of Uberlândia, Experimental Aerodynamics Research Center – CPAERO, Av. Joao Naves de Avila, 2121, Uberlandia – MG.
dennersavio@outlook.com
odenir.almeida@ufu.br

Abstract. *Landing gear (LG) is one of the dominant aircrafts drag and noise components at approach. Continued research efforts to reduce landing gear drag and noise are essential. This paper describes further development of a landing gear and presents results obtained from the wind tunnel testing of a simplified small-scale model nose landing gear. An Airbus A320 aircraft's typical configuration was selected as reference and a simplified LG was used as test-article. A nose landing gear was completely modeled using CATIA V5 and a 1/6 scaled landing gear model was used due to the size of the wind tunnel. The emphasis in this experiment was based on pressure distribution and velocity profiles behind the bluff body. Also, the aerodynamic drag coefficient has been evaluated in this work. Documented measures from other wind-tunnels have been taken for comparisons and verification of the experiment with computational fluid dynamics (CFD), through which there was an attempt to quantify the accuracy of our models, methods and assumptions. Despite the discrepancy in the Reynolds number, several results containing drag-coefficient, pressure distribution, velocity profiles and flow visualization are reported.*

Keywords: *experimental measurements; nose landing gear; bluff body; drag coefficient; aerodynamics.*

1. INTRODUCTION

Landing gear (Rajesh, 2015) is one of the important parts of an aircraft, often referred to as undercarriage, being a structure, which is installed on the aircraft for the purpose to support the weight of the aircraft while it is on the ground and allows the aircraft for smooth maneuver such as takeoff and landing. They also must be resistant to corrosion, stress corrosion, hydrogen embrittlement, and crack initiation and propagation. Landing gear also provides mobility to the aircraft on ground or water (Vilela, 2016). It can reach the largest local load on the plane. Fig. 1 illustrate the A380 nose landing gear configuration, with details for the nomenclature of parts.

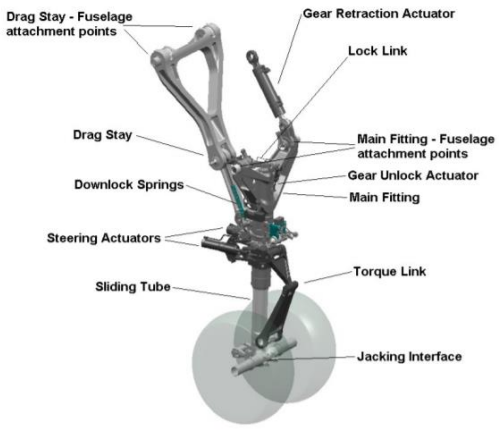

Figure 1. Airbus A380 nose landing gear. Source: Bernardini (2008).

Due to the increasing number of flights at airports worldwide, this has caused a steady increase in noise in these cities. More stringent legislation was created to reduce the amount of noise over cities around the world. Aircraft manufacturers were forced to initiate research, in which the focus would be the reduction of aircraft noise. Research started with tackling the most dominant component, engine noise (Boorsma, 2010). As a result, engine noise has been

reduced dramatically over the past decades, thereby increasing the relative importance of airframe noise for noise certification and environment considerations.

Landing gear noise can be the dominant component of airframe noise, especially for larger aircraft (Dobrzynski, 1997). In this case the total airframe noise can only be reduced significantly if all components are reduced by a similar amount, which makes reduction of landing gear noise essential. Purely designed to perform their main function, landing gears feature an extremely aerodynamically unfriendly shape. Due to this slightly aerodynamic geometry the interaction of airflow with protrusions and cavities gives rise to complex unsteady flow phenomena, constituting a powerful sound generating mechanism. So, landing gear produces noise at the same time drag.

The drag originating from the deployed landing gear of the aircraft is one of the significant contributors to overall airframe drag during aircraft approach (Eleonora, 2017). Making a good aerodynamic study is extremely important to the performance of an aircraft. This article will contribute to a nose landing gear analysis of a simplified nose landing gear, given that its geometry directly influences drag, aeroacoustic and pressure distribution.

At the present time it is common to find a range of articles with numerical analysis on nose landing gear, such as, LAGOON (Manoha et al., 2009), which analyzes aerodynamic experiments and initial aeroacoustic results. However, in relation to the experimental analysis it is very rare to find articles that discuss it. In engineering it is of great importance to confront numerical and experimental results. Therefore, this work aims to provide experimental data to be confronted with further numerical data (underway), generating more credibility to the study.

With the purpose of enriching the studies on experimental measurements in the flow on a simplified landing gear, this document presents selected data and of great relevance, considering all the difficulties to generate experimental data, such as the physical and digital construction of a model, access to equipment; wind tunnel, aerodynamic balance and pressure systems among other measurement accessories. The Lagoon nose landing gear used in this experiment was a 1:6 scale model which is based on the AirbusA320 aircraft. The nose landing gear was tested in the Experimental Aerodynamics Research Center (CPAERO) at Federal University of Uberlandia. The main purpose was to validate the measurements techniques and to generate a full set of aerodynamic data for further numerical analysis through computational fluid dynamics (CFD), currently being used at the Laboratory. Further details of the experimental setup and results are being presented concurrently with this paper.

2. METHODOLOGY

2.1 Mathematical equations

Velocity in a flow field is a very important quantity and could be evaluated through different approaches. As for instance, by using a Pitot tube it is possible to quantify the velocity magnitude by Eq.(1). Other possibilities are hot-wire anemometry, Particle Image Velocimetry (PIV) among others measurement techniques.

Pressure, by itself, is a dimensional quantity. However, in aerodynamics it is more plausible to work with dimensionless values. Such a quantity is the pressure coefficient (Cp), as described by Eq.(2). The pressure coefficient is a dimensionless number which describes the relative pressures throughout a flow field in fluid dynamics. The pressure coefficient at a point near a body is independent of body size. Consequently, an engineering model can be tested in a wind tunnel, pressure coefficients can be determined at critical locations around the model, and these pressure coefficients can be used with confidence to predict the fluid pressure at those critical locations around a full-size aircraft.

The drag coefficient (Cd) is a number used to model all the complex dependencies of shape, inclination, and flow conditions on aircraft drag. The equation of the drag coefficient (Eq.3) is simply a rearrangement of the drag equation where it is solved for the drag coefficient in terms of the other main flow variables.

$$V = \sqrt{\frac{2\Delta p}{\rho}} \tag{1}$$

$$cp = \frac{p - p_\infty}{\frac{1}{2}\rho V_\infty^2} \tag{2}$$

$$C_d = \frac{F_d}{\frac{1}{2}\rho V_\infty^2 A} \tag{3}$$

2.2 Small scale prototype

With the help of CATIA V5 R19® a simplified model of the landing gear was designed. The landing gear was a 1/6 scale model and it was based upon the LAGOON project (LAnding Gear NOise database for CAA validatiON) – Manoha et al. (2009). In Fig. 2 it is possible to visualize the simplified model in 2D views and its dimensions in millimeters. Following, the model was manufactured using a MakerBot® 3D printer with an ABS filament of 1.75 mm diameter, all the parts of the model were made separately, glued, covered with resin, painted and finally joined forming the final assembly. The final model 3D-sketched is illustrated in Fig 3.

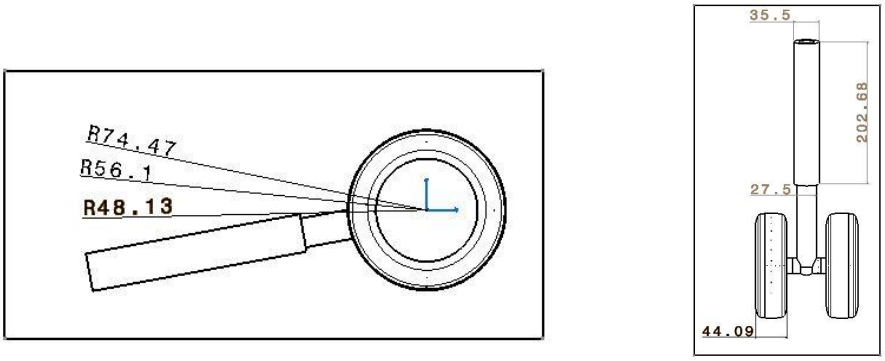

Figure 2. Test article dimensions (mm)

Fig. 3. Final landing gear model.

In Fig. 4 it is possible to visualize the simplified model and the real model used in the work of Manoha (2009), respectively.

(a) simplified model

(b) real model

Figure 4. Nose Landing Gear. (a) simplified model (b) real model – Manoha (2009)

The Lagoon was based on the design requirement, where the landing gear dimensions have been changed to suit the dimensions of the wind tunnel. The general dimensions of the model were chosen to be as large as possible with the constraint of a reasonable blockage coefficient at the closed test-section. There were two criteria to be met: the front area of the model should not occupy more than 10% of the flow section of the wind tunnel and there should be at least 10 cm between the model and the sidewalls. Which would mean a scale factor of 1/6 with respect to a nose landing gear of an Airbus aircraft. It was found that the distances of 10 cm in relation to the walls were being respected.

2.3 Experimental Setup

The Experimental Aerodynamics Research Center (CPAERO) at Federal University of Uberlandia offers complete support for experimental measurements of a small-scale prototype. The experiments were carried out in the 60 x 60 cm^2 wind tunnel (TV-60). The drive system of the wind tunnel comprises a 12-blade rotor driven by a 25 HP electrical engine responsible for creating the flow momentum in the tunnel. The flow velocity is driven by an electrical inverter which output varies from 0 to 60 Hz, which gives a flow velocity range from 0 to 28m/s. This subsonic wind tunnel is instrumented with pressure taps and analogic manometer. A Pitot tube and a digital manometer are used to calibrate the wind tunnel as well as to collect measured data in some experiments.

For the boundary layer profile assessment both multi-hole Pitot tube and hot-wire anemometry systems were available. For drag-force measurements 3-component and 6-component aerodynamic balances were available. Pressure distribution was achieved by a 64-channel pressure-transducer system and an Aeroprobe® 24-channel module and 5-hole Pitot tube. One of the experimental setups used in this research is sketched in Fig.5. A picture of the WT and its accessories are illustrated in Fig.6.

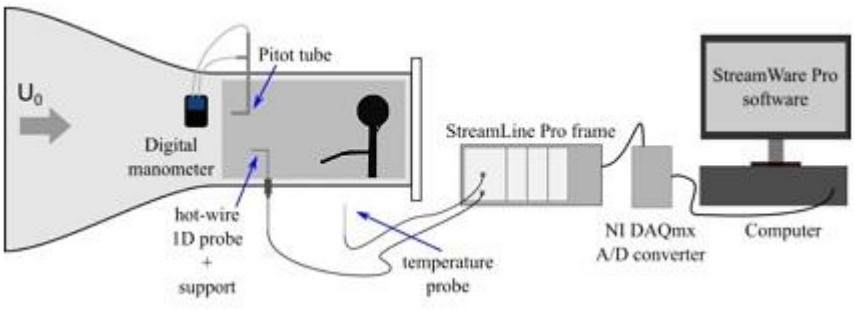

Figure 5. One of the laboratory setup used in this study.

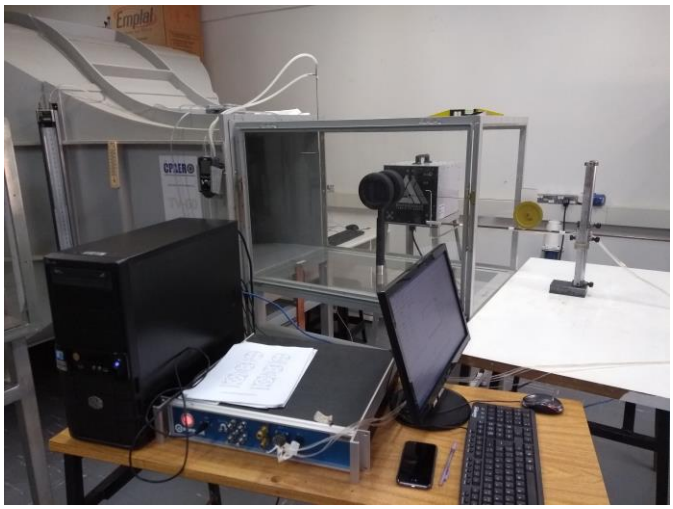

Figure 6. TV(60) with the Aeroprobe® 5-hole accessory.

Figure 7 shows the nose landing gear model fixed in the 3-component balance in the sidewall of the wind tunnel (TV-60).

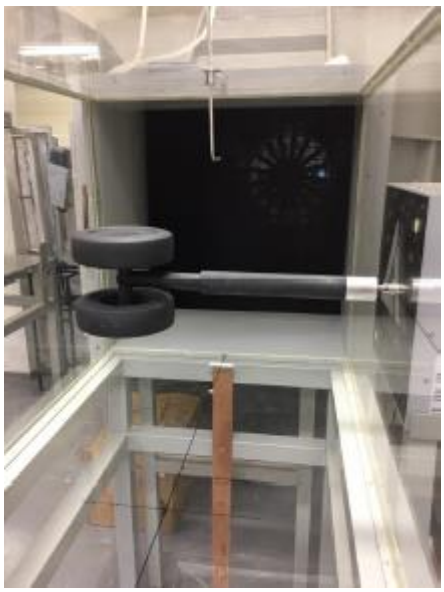

Figure 7. Wind Tunnel with the model fixed in the 3-component aerodynamic balance.

As reported by Almeida (2017), an improvement has been applied to this wind tunnel with inclusion of four wire-mesh screens and guide vanes after the fan, to straight the flow inside the channel. These modifications helped to decrease the turbulence intensity for levels around 0.5 – 0.8% inside the test section, providing a good flow quality with minimum distortion provided by the fan blades.

Another important quantity to be considered is the Reynolds number (Eq. 4). With the tabulated values of the air density and the dynamic viscosity as a function of temperature and pressure at infinity (freestream), respectively $\rho\ (T_\infty)$ and $\mu\ (T_\infty)$ and setting the flow velocity (V_∞) at operating condition of 16 m/s it was possible to calculate the value of the Reynolds number in function of the characteristic wheel-diameter D.

$$Re = \frac{\rho V D}{\mu} \tag{4}$$

For the current analysis the Reynolds number was of order 1.5×10^5, at least one order of magnitude less than those considered for real landing gear application. This is important to emphasize since Reynolds and Mach number are the governing parameters for such aerodynamic analysis i.e., the results are Re and M number dependent.

3. EXPERIMENTAL RESULTS

3.1 Boundary layer-profile

In order to measure the boundary layer profile of the wind tunnel used for this paper, an experiment was carried out in which the wind tunnel was set at a constant velocity of 16 m/s, the runoff was subjected to a room temperature of 26°C. With the aid of the pressure system and the anemometer it was possible to measure the pressure variation along the vertical position upstream the landing gear model, where the anemometer was displaced in the vertical direction of the wind tunnel. Given Eq. (1), the velocity was calculated. The graph of the profile of the boundary layer was plotted in Fig.8 where on the ordinate-axis is the displacement in (mm) and at the abscissa the velocity in (m/s). This result is in accordance with other measurements performed at the laboratory and consistent with data from Silva-Pinto (2016). The boundary layer profile would be helpful to be used in upcoming CFD simulations for this landing gear, since the upstream entry condition could be properly set in accordance with the wind tunnel measurement.

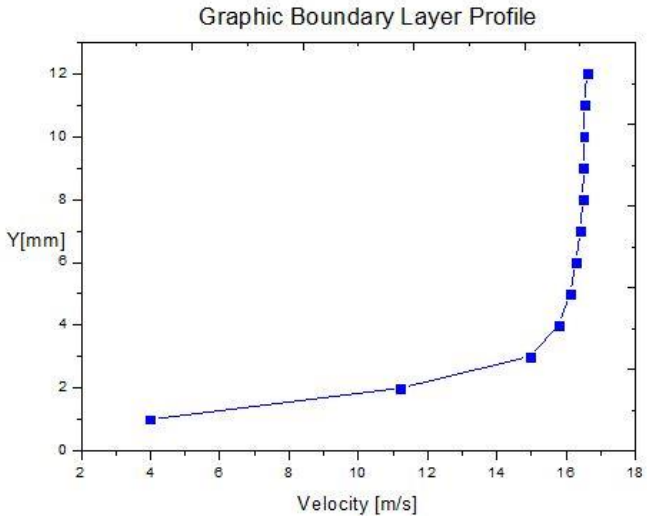

Figure 8. Graphic of the boundary layer profile.

3.2 Drag Coefficient

The experiment to obtain the drag coefficient was performed by configuring the wind tunnel at three different velocities varying from 12 m/s, 16 m/s and 20 m/s. The landing gear was fixed on the aerodynamic balance by means of a rigid screw-connection at the main axle of the balance. As the output of the aerodynamic balance was based on mass (kg), at the start of the test, the mass data was acquired by considering a row of measurements, e.g., at least three row of 10 measurements each, then the values were averaged, multiplied by the gravitational constant, and the drag force was obtained and consequently the drag-coefficient. The density was calculated based on the test-section temperature and pressure at which it was 27°C. The front area of the landing gear was calculated previously in the software Catia® and it was considered at the coefficient calculation. Fig. 9 presents the drag-coefficient curve (values) for the three tested-conditions.

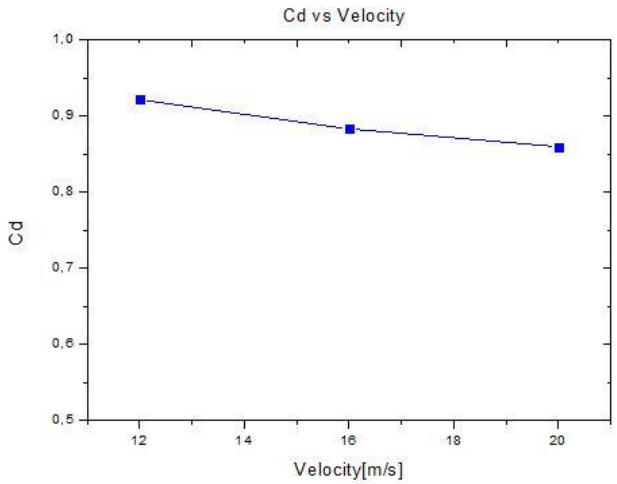

Figure 9. Graph of the Cd as a function of velocity by considering 3 test-points.

It should be noted that there is no other experimental data from this nose landing gear, at least registered in the opened literature. As mentioned before, the value of the drag coefficient is Reynolds dependent and these values must be compared with other experimental or numerical database, in order to check the levels and repeatability.

3.3 Pressure distribuition on the wheel

One of the wheels of the nose landing gear was instrumented with a pressure tap (0.8 mm diameter). As the wheel could be rotated, a graduated scale at angles of 20 degrees by 20 degrees was printed in the main axle. The internal hose was passed through the left wheel, junction and main leg leaving the wind tunnel section from the bottom of the test-section by means of a perforated connection (screw). Figure 10 illustrates the 3D-drawing for showing the hollow parts of the landing gear and the final assembly with the hose installed on in.

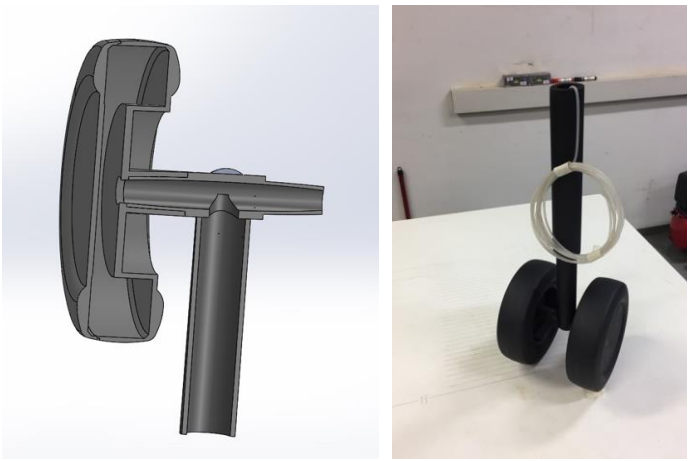

Figure 10. Experimental setup for wheel pressure measurement.

The following measurements were performed with a 64-channel pressure transducer module AA-TVCR2®. This module was designed to receive static pressure and total pressure (differential pressure). The differential pressure is then measured, having as the reference the static pressure inside the test-section. Before starting the acquisition a simple calibration check was performed by comparing the measurements taken by the module with a simple Pitot tube placed in the empty tunnel in the middle of the main stream and a static pressure tap on the wall, respectively in the same planes (perpendicular to the flow) as the total and static pressure jacks of a simple reference Pitot probe. With the appropriate pneumatic connections in the module, 5 different flow velocities, the set dynamic pressure values and the reference Pitot were observed. The values obtained with the module were all very close to 94% of the value of the Pitot system. This enabled us to conclude the reliability of the module for all channels.

The static pressure tap was already attached to the tunnel wall and the module's total pressure tap must be connected to the hose connected from the inside to the model wheel hole. The pressure taken on the wheel is unique, so the wheel angle was rotated from 0 ° to 360 ° by varying it in a step of 20°C, thus making measurements throughout its revolution. The aim was to take measurements with different angles, describing a complete rotation and thus having the pressure profile around the wheel, as if there were several holes on it. The results are shown below in the form of dimensionless pressure, i.e., the pressure coefficient Cp according to Fig.11.

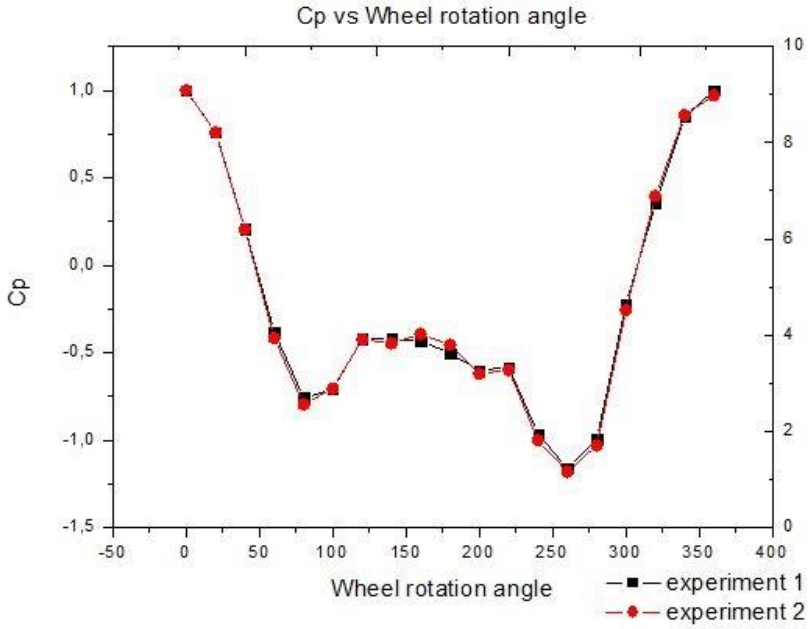

Figure 11. Wheel pressure distribution from 0° up to 360°.

The pressure distribution is quite consistent with the original work of Manoha et al. (2009), where the trend of the curve is kept almost the same with the levels for same angular position very similar. It is important to observe the two passages to 0 which roughly correspond to the positions 45 and 315 degrees, i.e., the positions of the hole in the static pressure outlet. This means that the current lines are tangent to the surface of the wheel. There are two local minimums at 80 and 260 degrees that indicate the presence of 2 boundary layer detachments at these locations. The profile of Cp around the wheel of the NLG and around a single cylinder are very similar. However, in the case of the cylinder, the

graph is symmetrical, whereas it is not the case of the wheel: the second local minimum is smaller than the first. This means that the cylinder can be associated with the wheel, the asymmetry of the Cp comes from the asymmetry of the rest of the model and, consequently, the turbulence generated by the axis of the support wheel and the central arm.

As mentioned, despite both Mach and Reynolds number differences, this work was aimed to provide the capabilities to experimentally assess the aerodynamics of a nose landing gear by providing data for further CFD simulations. It is believed that this goal has been achieved.

3.4 Preliminary Flow Visualization

In the original work of Manoha et al. (2009), due to the high Reynolds number flow, the authors illustrate the boundary layers transition by means of using artificial tripping. One of the motivations for doing that is to correctly provide data for CFD validation which requires to know the exact position of transition on the wheels and main axle and leg. Figure 12 presents some pictures form the work of Manoha et al. (2009), showing 4 successive acenaphthene visualizations to adjust position and nature of device – combination of zig-zag (on wheels) and cad-cut (on cylinders).

Figure 12. Boundary layer transition – artificial tripping, from work of Manoha et al. (2009).

In this work, a very simple technique of combining kaolin with kerosene – china clay method – was applied to the nose landing gear configuration in the wind tunnel at 16 m/s flow speed. As mentioned, no tripping device was applied, and the flow was kept uniform during the time from which the pictures were taken. Unfortunately, at the time of this visualization, there were no studio-lights for removing reflections and blurring from the pictures taken, so, a high quality was not properly achieved. However, some of the flow pattern over the wheel and main axle was possible to obtain. Figure 13 summarizes the preliminary flow visualizations gathered at the time of this work.

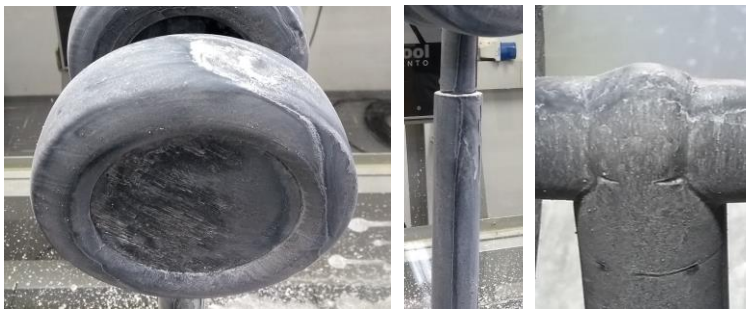

Figure 13. Preliminary flow visualization from China clay technique.

Despite the very simple technique, some characteristics of the flow pattern over the wheel, main leg and axle could be identified at the light of the results from Manoha et al. (2009). In addition, it helps to explain what was seen in the wheel pressure distribution. The large area between the two recesses at the rear of the landing gear is a low-pressure zone (lowest Cp's) what is responsible for the drag.

The boundary layer transition is commonly affected by upstream turbulence, roughness of the model surface, model orientation inside the test-section, model vibrational-modes among other variables. At this time, it is believed that a more dedicated work could be carried out to help better characterize the flow pattern over this nose landing gear. Results are given for just an overview of the phenomena.

4. CONCLUDING & REMARKS

This work was aimed to investigate the flow over a simplified nose landing gear and to validate the measurements techniques and to generate a full set of aerodynamic data for further numerical analysis through computational fluid dynamics (CFD), currently being used at the Laboratory. Based on the difficult of generating experimental data, such as the physical and digital construction of a model, access to equipment, wind tunnel, aerodynamic balance and pressure systems among other measurement accessories, this work has provided some results that could be helpful to enhance the capability of doing experiments at small scale wind tunnels. Results were expressed in terms of drag coefficient, wheel pressure distribution, boundary layer profile and flow visualization. The boundary layer profile was measured as a matter of providing upstream condition for CFD simulation. The nose landing gear drag evaluation for this model configuration was something new, since no other data was identified – so far – in the open literature. The wheel pressure distribution was consistent, as expected, the value of Cp did not exceed 1, since the maximum value is reached when the orifice is facing the flow. The flow visualization helped to confirm the pressure distribution over the wheel. Following, the next steps for this work would be the computational fluid dynamics (CFD) by considering steady-state and transient simulations and performing a complete analysis through comparisons with these data and complementary wind tunnel experiments that could be carried out by demand of the research.

5. ACKNOWLEDGEMENTS

The authors thank UFU for supporting the development of this work and for funding the participation on this event.

6. REFERENCES

Dobrzynski1 W., Leung C.C, Malcolm S., Antoine B., Olivier D., and Nicolas M., 2010, “Experimental assessment of low noise landing gear component design”, International Journal of Aeroacoustics, Vol. 9, No. 6, pp.763–786.

Eleonora Neri, John Kennedy, Gareth J. Bennett., “Bay Cavity Noise for Full-Scale Nose Landing Gear: A comparison between experimental and numerical results”. Aerospace Science and Technology”, Dublin- Ireland, 2017.

K. Boorsma, X. Zhang, N. Molin, Landing gear noise control using per-forated fairings, Acta Mech. Sin. 26(2) (2009) 159–174.

Manoha E., Jean B. and Vlad C., 2009, “LAGOON: further analysis of aerodynamic experiments and early aeroacoustics results”, 30th AIAA Aeroacoustics Conference. Miami, Florida

Rajesh A, BT Abhay, 2015, “Design and Analysis Aircraft Nose and Nose Landing Gear”, Journal of Aeronautics & Aerospace Engineering. Vol. 4, pp. 100014.

Almeida, O. and Pinto, W.J.G.S., 2017. “Experimental Analysis of the Flow Over a Commercial Vehicle – Pickup”. Universidade Federal de Uberlândia, Brasil.

Vilela A., Jansson N. and Hoffman J., 2016, “Computation of Aeroacoustic Sources for a Gulfstream G550 Nose Landing Gear Model Using Adaptive FEM”, Computers and Fluids.

7. RESPONSIBILITY NOTICE

The author(s) is (are) the only responsible for the printed material included in this paper.